

Full Length Research Paper

Characterization and Morphological Analysis of Biologically Synthesized Silver Nanoparticles

^{1,2}E.H. El- Mossalamy, ¹Abdullah Yousif Obaid, ¹L. M. Al-Harbi ³N.F. Al Harby
⁴A. A. Al-Owais and ⁵Zaheer Khan

¹Department of Chemistry, Faculty of Science, King Abdulaziz University, P.O. Box 80203, Jeddah 21589, Saudi Arabia ²Chemistry Department, Faculty of Science, Benha University, Benha Egypt ³Chemistry Department, Faculty of Science and Arts, Al Qassim University. Saudi Arabia

⁴Chemistry Department, King Saud University, P.O.Box 272047, Riyadh-11352, Saudi Arabia.

⁵Department of Chemistry, Jamia Millia Islamia (Central University), New Delhi-110025, India

Accepted 15 October, 2013

The effect of cetyltrimethylammonium bromide, CTAB has been studied on the optical properties and morphology of advanced Ag-nanoparticles (AgNPs) using *Oriental plane* leaves extract as a reducing-, stabilizing- and capping-agent for the first time. The formation of AgNPs was monitored by measuring the UV-vis. spectra at different time intervals (5, 10, 20 and 30 min) after adding the leaves extract (from 1 to 5 cm³) to the different AgNO₃ solutions ([Ag⁺] = 4.0, 8.0, 12.0, 16.0 × 10⁻⁴ mol dm⁻³). The sigmoidal nature of the reaction- time plots suggests the involvements of an autocatalytic reaction path. In presence of CTAB, the peak at 450 nm is shifted to shorter wavelength, i.e., 425 nm and sharpness of the surface resonance plasmon (SRP) band also decreases. The results confirm a significant change in the morphology and/or agglomeration tendency with CTAB. Transmission electron microscopy (TEM) results show the formation of stable AgNPs at different concentration of AgNO₃ gives mostly spherical particles with diameter ranging from 10 to 30 nm.

Keywords: Oriental plane; Silver particles; CTAB; Morphology.

INTRODUCTION

Cetyltrimethylammonium bromide exhibits a number of role in the synthesis of spherical, nonspherical (wires/rods, disks, sheets/plates, cubes, prisms, hollow structures, multi-branched and/or multi-pods metallic gold and silver nanoparticles (Chen et al., 2003). Generally, the use of polymers, ligands, solid matrix and surfactants has also been suggested to the stabilization of small nanoparticles.

In this content, surfactant aggregates, especially micelles, reverse micelles and macroemulsions, will get an edge over other stabilizers (Pileni 1993). It has been established that a surfactant, especially CTAB, is required as a shape-directing agent in the all syntheses of branched metal nanostructures (Lou et al., 2006). Aqueous solutions of surfactants have been known to exhibit unusual properties. At low concentrations, it behave just like an ordinary electrolytes, but after attaining a certain concentration surfactant chains tend to self-associate, resulting in the formation of various aggregates (micelles, microemulsions,

*Corresponding Author's Email:
sbdmina@yahoo.com; Tel:+20-1009143680.

vesicles) (Fendler 1982). Reduction ability of natural plants extract came directly from the various constituents containing $-NH_2$, $-COOH$, $-OH$, $-SH$, etc, groups. The role and use of shape-directing cetyltrimethylammonium bromide in the similar investigations involving greener reducing agents has been neglected (Khan et al., 2012). Jose-Yacaman et al. (Gardea-Torresdey et al., 2002). prepared the gold and silver nanoparticles by using living plants for the first time. Very recently, the literature is replete with the investigations of the use of natural products (azadirachta indica leaf broth (Shiv Shankar et al., 2004), aloe vera plant extract (Chandran et al., 2006), camellia sinensis (Vilchis-Nestor et al., 2008), lemongrass leaves extract (Shankar et al., 2005), natural rubber (Abu Bakar 2007), starch (Vigneshwaran et al., 2006), sesbania drummondii (Sharma et al., 2007), seed extract of jatropha curcas (Bar et al., 2009), nyctanthes arbortristis flower extract (Das et al., 2011), as a alternate source of the toxic reductants.

In this article, we describe a one-pot chemical reduction method to the formation of AgNPs using aqueous leaves extract of *Oriental plane*, is large, deciduous tree of the Platanaceae family. The leaves of *Oriental plane* are used for the treatment of astringent, dysentery, heal wounds, chilblains and ophthalmia. Large number of molecules such as platanin, tannin, allantoin (diureide of glyoxylic acid), phlobaphene (insoluble phenolic substances), mannitol (sugar alcohol; osmotic diuretic agent and a weak renal vasodilator), platanolic acid (hydroxy-carboxylic acid), and platanol are the bioactive constituent of chinara leaves. Keeping in view the role of citric acid, ascorbic acid, sugars and amino compounds [8] for the synthesis of advanced AgNPs we are interested in developing a 'green' route to synthesize AgNPs using *Oriental plane* leaves extract as reducing as well as capping agent. Therefore, this study aims at exploring the possibility of synthesizing AgNPs using a bio-chemical reduction method and CTAB (a shape-directing stabilizer) under normal atmospheric conditions. To the best of our knowledge, this is the first ever report on *Oriental plane*-assisted green synthesis of AgNPs. In addition, the shape-directing role of CTAB surfactant has also been studied and discussed in details. In the present study, we show that an extract of *Oriental plane* leaves placed in an aqueous solution of $AgNO_3$, resulted in the reduction of the Ag^+ ions and formation of stable AgNPs. The method is simple, clean and the required only reactants (extract and $AgNO_3$) and water, this method has an advantage in higher scale production of AgNPs over the chemical and physical methods.

MATERIALS AND METHODS

Synthesis of silver nanoparticles

To the preparation of aqueous solution of chinara leaves

extract, 10 g fresh leaves collected from the Srinagar, Jammu and Kashmir, India, perfectly washed, chopped in to small pieces and added to a Borosil conical flask containing 250 ml double distilled deionized water. The reaction mixture was kept on a boiling water bath for 30 min, cooled and filtered it through What-man filter paper no. 40. The perfect transparent clear filtrate contains only soluble organic moieties of the chinara leaves and the solid residue is discarded. This resulting aqueous solution used for the reduction of Ag^+ ions to the metallic Ag. A fresh stock solution of $AgNO_3$ (Molecular weight: 169.87 g/mol, assay: 99%: Merk India) was prepared by dissolving requisite solid $AgNO_3$ in double-distilled water. Exactly 5.0 cm³ of the extract was added to 50 cm³ reaction mixture (0.01 mol dm⁻³; 8.0 cm³ $AgNO_3$ + 37 cm³ water) in a 250 ml Borosil flask and kept it at room temperature for the reduction process. As the reaction time increases, appearance of pale-yellow observed which indicating the formation of AgNPs (Al-Thabaiti et al., 2008).

Characterization of silver nanoparticles

The appearance of silver sol (reduction of Ag^+ ions by leaves extract) was monitored by UV-vis spectroscopy (Shimadzu UV-Vis spectrophotometer; model UV-1800, Japan) as a function of time by using a quartz cuvette with water as reference. The morphology of AgNPs was examined using TEM image of the sample was obtained using Hitachi 7600 with an accelerating voltage of 120 kV. The selected area electron diffraction (SAED) data were also recorded. Sample for TEM analysis were prepared by coating of aqueous AgNPs drops on carbon-coated copper grids, kept for 5 min; the extra solution was removed using blotting paper at room temperature.

RESULTS AND DISCUSSION

Visual observations and U.V.-vis spectra

A preliminary visual observation shows that the initial color of the reaction mixture after the addition of leaves extract to the aqueous $AgNO_3$ solution was nearly colorless. Interestingly, the color of the reaction mixture changed from pale-yellow, pink-yellow, light brown, wine-red to dark brown exponentially with reaction-time as aggregation proceeds. Colourlessness of reaction mixture at the initial stage and the final deep reddish-brown color after the completion of the reaction are shown in (Figure. 1), which indicating that the AgNPs shape, size and the size distribution altering with the reaction time at different stages (Khan et al., 2012). The color change might be due to the excitation of SPR in the production of AgNPs (Mulvaney 1996). The spectra of the biosynthesis production of AgNPs are noted at different time intervals and are shown in the Figure. 2 for the 5.0 cm³ of leaves

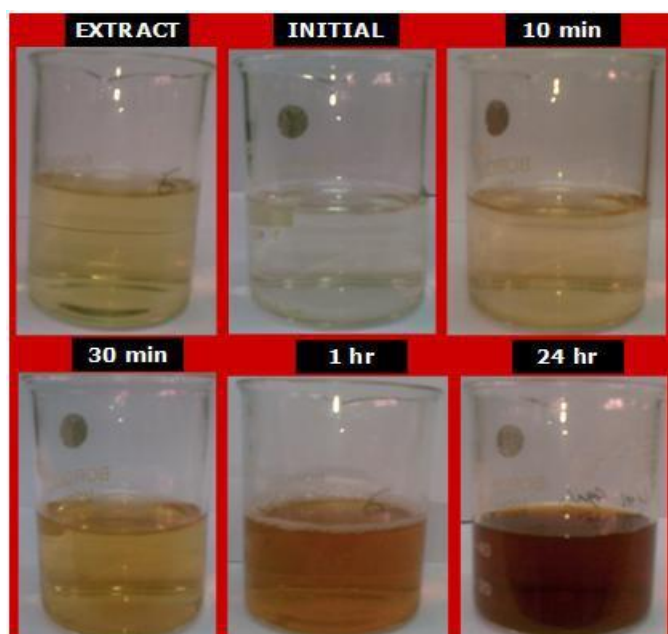


Figure 1. Optical images of chinnar leaves extract and its reaction product with AgNO_3 at different time intervals. *Reaction conditions:* $[\text{Ag}^+] = 16.0 \times 10^{-4} \text{ mol dm}^{-3}$, $[\text{extract}] = 5.0 \text{ cm}^3$, Temperature = 30°C .

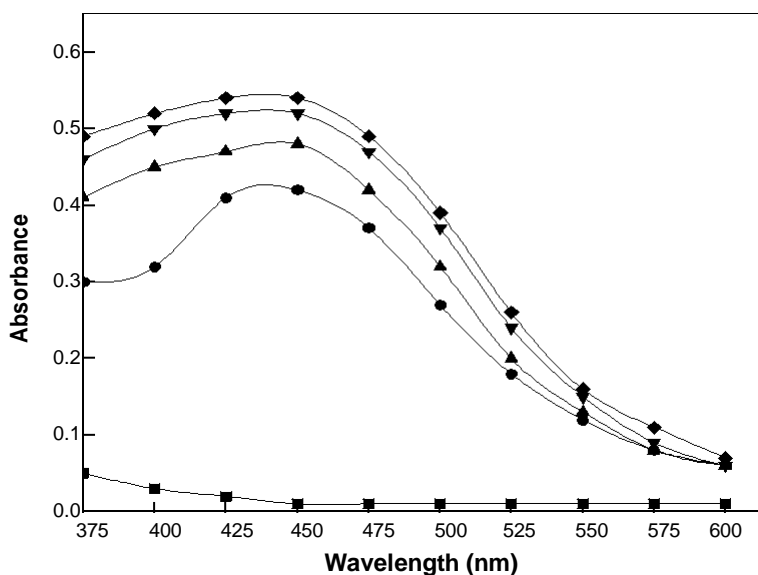


Figure 2. UV-vis bioreduction kinetics of the reaction of *Oriental plane* leaves extract with aqueous AgNO_3 with different time intervals. *Reaction conditions:* $[\text{Ag}^+] = 16.0 \times 10^{-4}$, $[\text{extract}] = 5.0 \text{ cm}^3$, (■), Time = 5 (●), 10 (▲), 20 (▼) and 30 min (◆).

extract. The SRP peak observed at 450 nm confirms the influence of aqueous chinnar leaf extract in reducing Ag^+ ions to AgNPs from aqueous AgNO_3 solution. Absorbance intensity of broad SRP band increases steadily as a function of reaction time. A weak absorbance peak was observed at 450 nm with 1.0 cm^3 of extract after 5 min. Interestingly, the position of the maximum absorption was

shifted to a shorter wavelength (from 450 to 425 nm; blue shift). Sharpness of the peak increases with time indicating that much smaller AgNPs were generated time (Figure. 3). In addition of a sharp peak at 425 nm, a weak shoulder also developed at 475 which might be due to the anisotropic growth of AgNPs. The broadness of the peak indicates the wide size distribution of the nanoparticles in

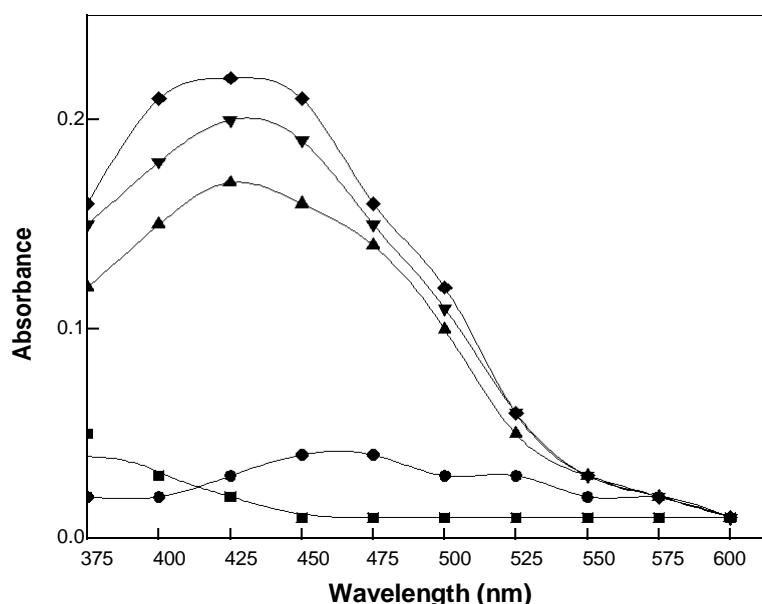


Figure 3. UV-vis bioreduction kinetics of the reaction of *Oriental plane* leaves extract with aqueous AgNO_3 with different time intervals. Reaction conditions: $[\text{Ag}^+] = 16.0 \times 10^{-4} \text{ mol dm}^{-3}$, $[\text{extract}] = 1.0 \text{ cm}^3$; (■), Time = 5 (●), 10 (▲), 20 (▼) and 30 min (◆).

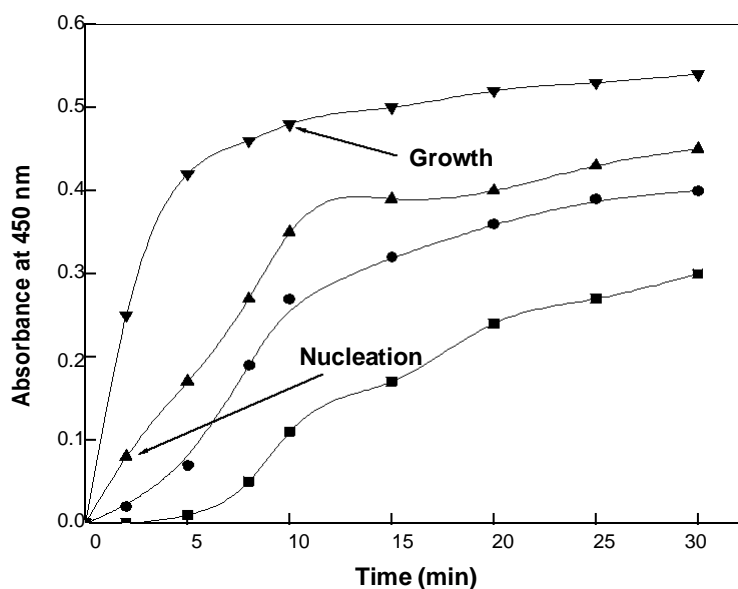


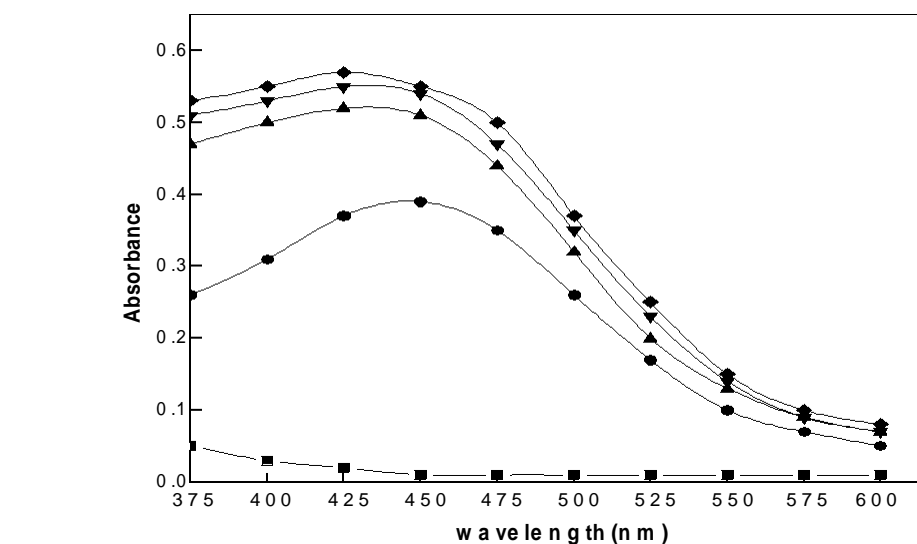
Figure 4. Reaction-time curves showing the effect of $[\text{Ag}^+]$ on the nucleation and growth of Ag-nanoparticles at room temperature . Reaction conditions:

the biomolecules constituents of leaves extract (Song and Kim 2009).

Kinetics and mechanism

The reaction-time curves shows that the Ag^+ ions reduction into Ag^0 occurs very rapidly and more than 90% of the

reduction of Ag^+ ions will be completed in 10 min. From 10 to 30 min, the reaction stops as the intensity of the reaction shows almost a parallel line with x-axis with respect to time (Figure. 4). No appreciable change in absorbance was noticed after 10 min for all the $[\text{Ag}^+]$ used in the entire study, confirming the complete reduction of Ag^+ ions to AgNPs. The sigmoidal shape of the reaction-time curves clearly suggests that autocatalysis was involved in the path



(A)
(B)

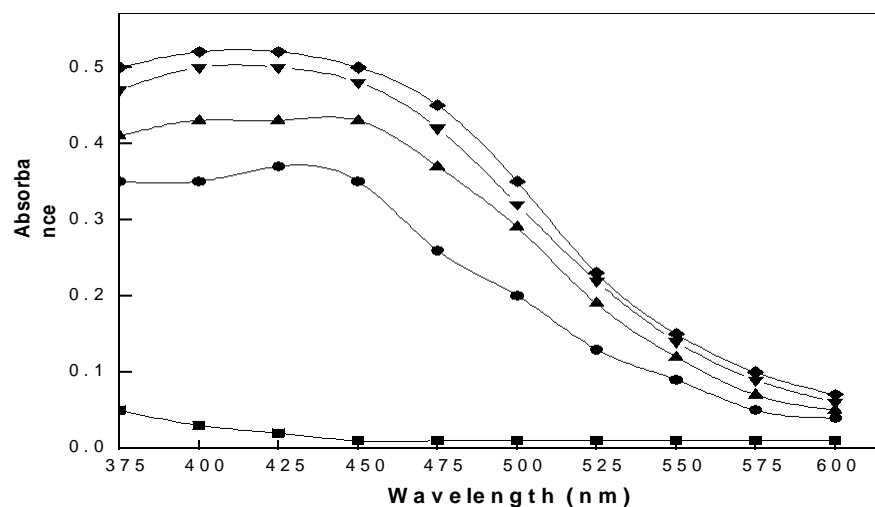


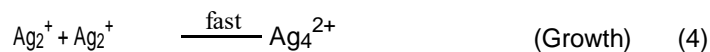
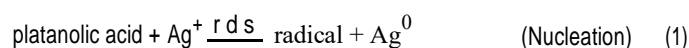
Figure 5. Absorption spectra of extract (■) and its reaction product with $[Ag^+] (= 16.0 \times 10^{-4} \text{ mol dm}^{-3})$ as a function of time. Reaction conditions: $[CTAB] = 4.0$ (A) and $8.0 \times 10^{-4} \text{ mol dm}^{-3}$ (B); $[extract] = 5.0 \text{ cm}^3$, Time = 5 (●), 10 (▲), 20 (▼) and 30 min (◆).

of AgNPs formation (Huang et al., 1993). Surprisingly, formation of transparent pale yellow color silver sol was not observed at lower $[Ag^+] (\leq 2.0 \times 10^{-4} \text{ mol dm}^{-3})$ where as, yellowish-white precipitate was also formed at higher $[Ag^+]$. Therefore, it can now be stated confidently that formation of AgNPs is not directly proportional to the $[Ag^+]$; small $[Ag^+]$ being enough to initiate the formation of metal

nucleation center which acts as a catalyst for the reduction of other Ag^+ present in the reaction mixture.

Hydroxy groups of reducing sugars and/or platanolic acid reduce Ag^+ into Ag^0 (Eq.1; rate-determining step, rds). The neutral atom Ag^0 reacts with Ag^+ to form the relatively stabilized Ag_2^+ clusters as shown in Eq.(3). Ag_2^+ clusters dimerize to yield Ag_4^{2+} (yellow-color silver sol; stable

species for along time in presence of a polyanion even under air and growth stops at the stage of this species (Eqs.(4) (Henglein 1993). The intervention of free radical were detected by adding acrylonitrile as a scavenger, the formation of white precipitate (Signorella et al., 1996), appeared slowly as the reaction proceeded indicating in situ generation of free radicals. Control experiments with Ag^+ ions and leaves extract did not show formation of a precipitate. On the basis of above results and discussion, Scheme 1 mechanism to the reduction of Ag^+ ions by constituents of chinnar leaves extract is proposed.



Shape-directing effect of CTAB

Surfactants are the amphiphilic molecules, which create highly anisotropic interfacial regions lining the boundary formed by the highly polar aqueous and nonpolar hydrocarbon regions. Micelles, dynamic aggregates can alter morphology and other surface optical properties to different extent depending up on their nature of head group, type of counter-ions and length of hydrophobic tail (Yu and Yam 2004). Bakshi and his co-workers (Bakshi 2010), used different surfactants, anionic, cationic and Gemini to the synthesis of multi branched advanced Ag and Au NPs and reported these stabilizers acted as a shape-directing agents. In order to see insight into the sub- and post- micellar role of shape-directing CTAB, a series of experiments were performed at two different [CTAB] i.e. 5.0×10^{-4} and 8.0×10^{-4} mol dm⁻³ at fixed concentrations of other reagents. The observed results are summarized in Figure. 5 as absorbance-wavelength profiles. The intensity of the SRP band was increased rapidly with time. However, the position of the maximum absorption was shifted to a shorter wavelength with the variation of reaction-time, indicating that much smaller AgNPs were generated in presence of CTAB. The peak at short wavelength may be attributed to the out-of plane quadrupole (Jin et al., 2001). In the present study, we did not observe any significant effect of sub- and post-micellar [CTAB].

TEM images and SADE patterns

Figure. 6 shows typical TEM images and SADE ring patterns of AgNPs prepared in absence and presence of CTAB using chinnar leaves extract. These results suggests that the obtained AgNPs were mostly irregular and agglomerated in a unsymmetric manner on to the surface of Ag^0 , reduction species of Ag^+ , with a larger size of 30 nm (Figure. 6 A). The reason for the aggregation is due to the presence of excess amounts of reducing moieties. The TEM analyses corroborates well with the results drawn from the corresponding reaction-time curves (Figure. 3).

Diffraction rings can be seen when corresponding selected area electron diffraction of AgNPs was conducted (Figure. 6B), which also corroborate the small size and crystalline nature of the silver nanoparticles by the appearance of lattice fringes similar to a lattice spacing {1.1.1} of bulk silver metal (Shankar et al., 2004). In presence of CTAB, the interactions and solubilization of reducing molecules occurs with the positive head group of CTAB. The AgNPs are also adsorbed and/or bound with the CTAB, which in turn, altered the morphology drastically and the number of spherical shaped AgNPs was also increased (Figure. 5C).

TEM micrographs clearly indicate the presence of coatings surrounding the AgNPs which might be due to the terpenoids and/or reducing sugars present in the leaves extract acted as a reducing- and capping-agents (Shankar et al., 2004). Figure 6C indicates that the AgNPs aggregated and/or deposited in a symmetric manner, resulted to the formation of beautiful silver (tiles-like structures with dimensions between 8 and 40 nm). The typical selected-area diffraction pattern are shown in Figure. 6D. The rings patterns are consistent with the plane families {110}, {111}, {200}, {220}, {311}, {331} and {422}, of pure face-centred cubic silver structure (Huang and Yang 2008; Guzman et al., 2008).

CONCLUSIONS

We have used *Oriental plane* leaves extract for the biogenic reduction of Ag^+ ions for the first time. The morphology (particle size and shape), shape of the spectra (intensity of peak and position of SRP band) and the stability of the resulting AgNPs are highly dependent on the concentration of AgNO_3 , leaves extract, CTAB, and pH. Platanolic acid (hydroxy carboxylic acid, triterpene) of chinnar leaves extract were mostly responsible for the reduction of silver ions to nanosized silver particles. TEM images show the ring of bilayer on the surface of the AgNPs. UV-vis spectroscopic data exhibits blue-shift of the SPR band with reaction time. AgNPs remain stable in the presence of high concentrations of leaves extract. The present method may be helpful in the development of similar stable systems with other metal nanoparticles.

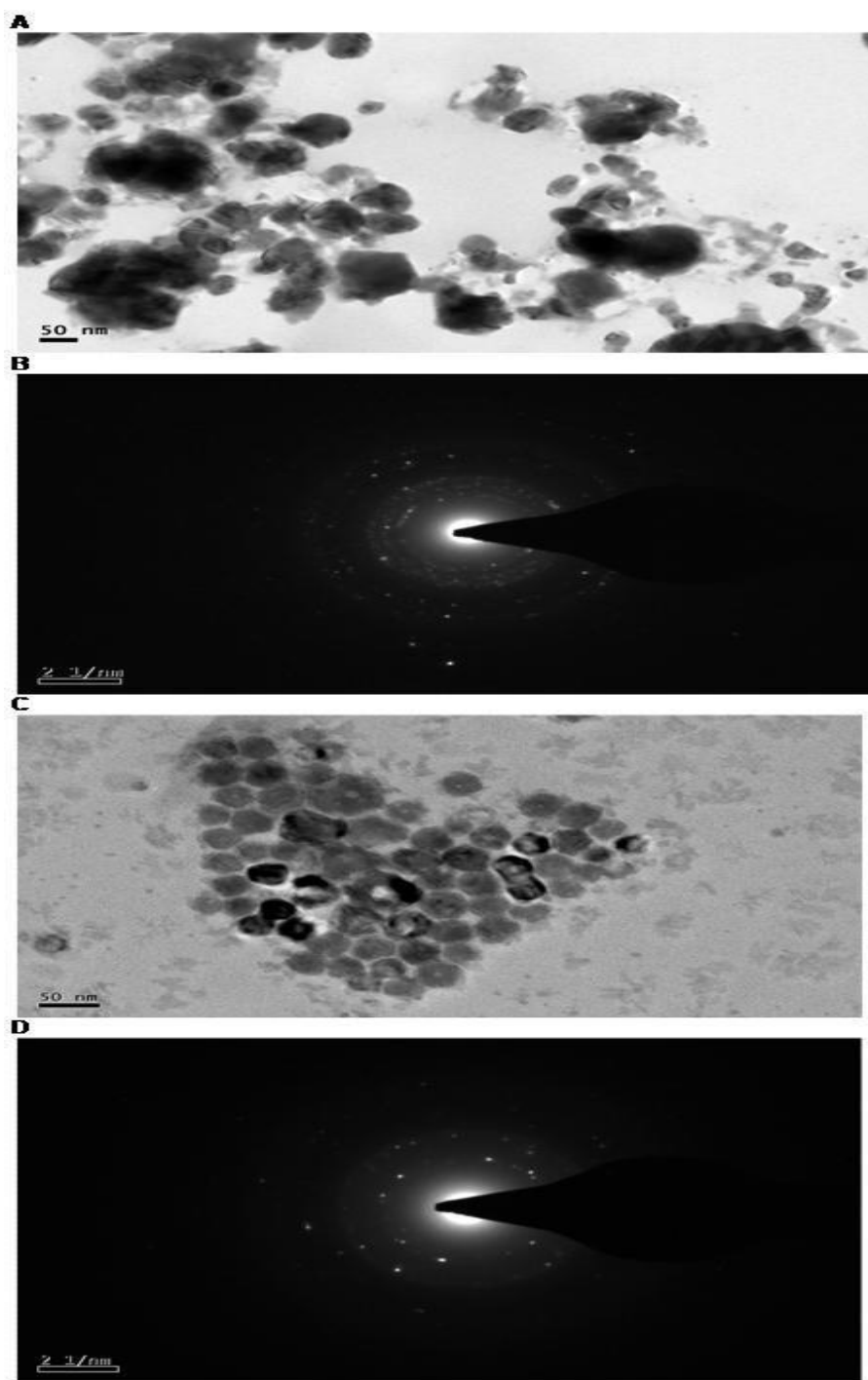


Figure 6. TEM images and SAED patterns of AgNPs synthesized using chinarr leaves extract (5.0 cm^3) in absence (A and B) and presence of CTAB (C and D).

ACKNOWLEDGMENT

This project was funded by the Deanship of Scientific Research (DSR), King Abdulaziz Univeristy, Jeddah, under

grant no.(1433 /130 /391). The authors, therefore, acknowledge with thanks DSR for technical and financial support.

REFERENCES

- Abu Bakar NHH (2007). J. Ismail, M. Abu Bakar, Mater. Chem. Phys. 104 (2007) 276;
- Al-Thabaiti SA, Al-Nowaiser FM, Obaid AY, Al-Youbi AO, Khan Z (2008). Colloids Surfs., B: Biointerfaces, 67 (2008) 230;
- Bakr OM, Wunsch BH, Stellacci F (2006). Chem. Mater. , 18 (2006) 3297.
- Bakshi MS (2009). Langmuir 25 (2009) 12697.
- Bakshi MS (2009). Langmuir 25 (2009) 12697.
- Bakshi MS (2010). J. Nanoscience Nanotechnology 10 (2010) 1757; Bar H, Bhui DK, Sahoo GP, Sarkar P, Pyne S, Misra A (2009). Colloids Surfs. A: Physicochem. Eng. Aspects 348 (2009) 212; Bunton CA (2006). Ad. Colloid Interface Sci., 123 (2006) 332.
- Chandran SP, Chaudhary M, Pasricha R, Ahmad A, Sastry M (2006). Biotechnol. Prog. 22 (2006) 577;
- Chen SH, Wang ZL, Ballato J, Foulger SH, Carroll DL (2003). J Am. Chem. Soc., 125 (2003) 16186;
- Das RK, Gogoi N, Bora U (2011). Bioprocess Biosyst Eng 34 (2011) 615.
- Fendler JH (1982). Membrane Mimetic Chemistry, Characterizations and Applications of Micelles, Microemulsions, Monolayers, Bilayers, Vesicles, Host-Guest Systems and Polyions, Wiley, NY, 1982;
- Gardea-Torresdey JL, Gomez E, Peralta-Videa J, Parsons JG, Troiani HE, Jose-Yacaman M (2003). Langmuir 19 (2003) 1357.
- Gardea-Torresdey JL, Parsons JG, Dokken K (2002). J. Peralta-Videa, H.E. Troiani, P. Santiago, M. Jose-Yacaman, Nano Lett. 2 (2002) 397;
- Guzman MG, Dille J, Godet S (2008). World Aca. Sci. Eng. Technolo., 43 (2008) 357.
- Henglein A (1993). J. Phys. Chem., 97 (1993) 5457.
- Huang H, Yang Y (2008). Composites Sci. Technolog., 68 (2008) 2948.
- Huang Z-Y, Mills G, Hajek B (1993). J. Phys. Chem. 97(1993) 11542;
- Hussain JI, Talib A, Kumar S, Al-Thabaiti SA, Hashmi AA, Khan Z (2011). Colloids Surfs., A: Physicochem. Eng. Aspects, 381 (2011) 23;
- Jin RC, Cho YW, Markin CA, Kelly KL, Schatz GC, Zheng JG (2001). Science 294 (2001) 1901;
- Kelly KL, Coronado E, Zhao LL, Schatz GC (2003). J. Phys. Chem. B 107 (2003) 668.
- Khan Z, Talib A (2010). Colloids Surfs., B: Biointerfaces, 76 164-169 (2010) 164;
- Khan Z, Al-Nowaiser F (2011). J. Dispersion Sci. Technolo., 32 (2011) 1665;
- Khan Z, Al-Thabaiti SA, Obaid AY, Khan ZA, Al-Youbi AO (2012). J. Colloid Interface Sci., 367 (2012) 101;
- Khan Z, Bashir O, Hussain JI, Kumar S, Ahmad R (2012). Colloids Surfs., B: Biointerfaces, 98 (2012) 85;
- Khan Z, Hussain JI, Hashmi AA (2012). Colloids Surfs., B: Biointerfaces, 95 (2012) 229;
- Khan Z, Singh T, Hussain JI, Hashmi AA (2013). Colloids Surfs., B: Biointerfaces, 104 (2013) 11.
- Kuo C-H, Huang MH (2005). Langmuir 21 (2005) 2012;
- Lou XW, Yuan C, Archer LA (2006). Chem. Mater. , 18 (2006) 3921;
- Mehta SK, Chaudhary S, Gradzielski M (2010). J. Colloid Interface Sci. 343 (2010) 447.
- Mulvaney P (1996). Langmuir, 12 (1996) 788.
- Pal T, Sau TK, Jana NR (1997). Langmuir , 13 (1997) 1481.
- Pileni MP (1993). J. Phys. Chem., 97 (1993) 6961.
- Rafey A, Shrivastav KBL, Iqbal SA, Khan Z (2011). J. Colloid Interface Sci., 534 (2011) 190;
- Rai A, Singh A, Ahmad A, Sastry M (2006). Langmuir, 22 (2006) 736.
- Sau TK, Murphy CJ (2004). J. Am. Chem. Soc. 126 (2004) 8648;
- Serra A, Filippo E, Re M, Palmisano M, Vittori-Antisari M, Buccolieri A, Manno D (2009). Nanotechnology, 20 (2009) 165501.
- Shankar SS, Rai A, Ahmad A, Sastry M (2004). J. Colloid Interface Sci., 275 (2004) 469;
- Shankar SS, Rai A, Ahmad A, Sastry M (2005). Chem. Mater. 17 (2005) 566;
- Sharma NC, Sahi SV, Nath S, Parsons JG, Gardea-Torresdey JL, Pal T (2007). Environ. Sci. Technol. 41 (2007) 5137;
- Shiv Shankar S, Rai A, Ahmad A, Sastry M (2004). J. Colloid Interf. Sci. 275 (2004) 496;
- Signorella S, Rizzotto M, Daier V, Frascaroli MI, Palopoli C, Martino D, Bousseksou A, Sala LF (1996). J. Chem. Soc. Dalton Trans., 1607 (1996).
- Song JY, Kim BS (2009). Bioprocess Biosyst. Eng. 32 (2009) 79.
- Tascioglu S (1996). Tetrahedron, 52 (1996) 11113; Tondre C, Hebrant M (1997). J. Mol. Liq., 72 (1997) 279;
- Vigneshwaran N, Nachane RP, Balasubramanya RH, Varadarajan PV (2006). Carbohydr. Res. 341 (2006) 2012;
- Vilchis-Nestor AR, Sanchez-Mendieta V, Camacho-Lopez MA, Gomez-Espinosa RM, Camacho-Lopez MA, Arenas-Alatorre JA (2008). Mater. Lett. 62 (2008) 3103;
- Yu D, Yam VW-W (2004). J. Am. Chem. Soc., 126 (2004)13200;
- Zaheer Z (2013). Rafiuddin, Colloids Surfs., B: Biointerfaces, 108 (2013) 90-94.